ELSEVIER

International Journal of Solids and Structures 41 (2004) 4163–4177

INTERNATIONAL JOURNAL OF SOLIDS and STRUCTURES

www.elsevier.com/locate/ijsolstr

An explanation for the minimal effect of body curvature on hypervelocity penetration hole formation

Lawrence J. De Chant *

Sandia National Laboratories, Thermal Reactive Processes, P.O. Box 5800, Albuquerque, NM, 87185-0825, USA

Received 29 July 2003; received in revised form 20 February 2004
Available online 27 March 2004

Abstract

Though not discussed extensively in the literature, it is known among workers in impact and penetration dynamics, e.g. the CTH analysis and development team at Sandia National Laboratories, that curvature of thin plates has a minimal effect on the penetration hole diameter due to a hypervelocity impact. To understand why curvature introduces a minimal effect on penetration hole size we extend a flat plate penetration hole diameter relationship (De Chant (2004a) Unpublished manuscript; De Chant (2004b) Mechanics of Materials, in press) to include the effect of body curvature. The effect of the body curvature on the hole diameter is shown to scale according to the dimensionless plate thickness to radius of curvature of the body i.e. h/R, which is typically small. Indeed for most problems where a single layer shell (plate) can be meaningfully defined, the effect of curvature upon hole diameter is on the order of other uncertainties in the problem, e.g. doubts concerning the appropriate equation of state and strength model, and is often, therefore, negligible.
Published by Elsevier Ltd.

Keywords: Curvature; Penetration hole diameter

1. Introduction

Hypervelocity plate penetration hole diameter prediction is of fundamental importance for a wide range of military and space applications (Piektukowski, 1999; Corbett et al., 1996). Although many of the applications associated with high-speed impact involve impact and penetration of cylindrical shells or pipes, few researchers include the effect of body curvature in their models since experience indicates that body curvature has a minimal effect on penetration hole size. To gain a sense of the type of problem where curvature is fundamental to the geometry of a problem, but are unclear as the effect curvature may have on penetration hole behavior, we consider an example computation performed using CTH (McGlaun et al.,

* Tel.: +1-505-844-4250; fax: +1-505-844-4523.
E-mail address: ljdecha@sandia.gov (L.J. De Chant).

0020-7683/$ - see front matter Published by Elsevier Ltd.
doi:10.1016/j.ijsolstr.2004.02.053

Nomenclature

C_f	hydrodynamic skin friction coefficient
c_{wave}	material sound speed
c_1, c_2, c_3	integration constants
d	projectile diameter
d_{hole}	finite thickness plate hole diameter
$f(y)$	"y" varying similarity separation function
h	plate thickness
m	hydrodynamic boundary layer exponent
R	radius of curvature
t	time
u	velocity in penetration direction
U	projectile impact velocity
U_b	Bernoulli velocity
u_τ	shear velocity
v	transverse velocity
y_{crit}	location of penetration hole edge from centerline
x	penetration direction coordinate
y	transverse directional coordinate
Y_{yield}	yield stress
α	wave damping term; C_f/h
ε_h	perturbation parameter, h/d
ε	curvature dependent term in y_{crit} equation; $\frac{1}{\left(\frac{U}{c_{wave}}\right)^{-1/2}\frac{R}{h}+1} \equiv \varepsilon$
ν	hydrodynamic kinematic viscosity
ν_{eff}	non-linear kinematic viscosity model; $\nu_{eff} = U/\alpha$
ρ_{proj}	projectile density
ρ_{targ}	target density
ψ	stream function

1990; Bell et al., 2000). Fig. 1 provides a comparison between (a) a 1 cm diameter 6061-T6 aluminum sphere impacting a 8 cm diameter, 0.23 cm thick hollow 6061-T6 aluminum sphere and (b) a 1 cm diameter aluminum sphere impacting a 0.23 cm thick plate computed using the adaptive grid refinement AMR version of CTH (Bell et al., 2000).

Though qualitatively we note that the penetration holes in Fig. 1 appear equivalent, it is not clear if this equivalence is a quantitative result and, moreover, if it is a general trend.

To study this problem and answer these questions we propose to develop an extension to a closed form analytical model developed by De Chant (2004a,b), and Appendix A, to include the effects of body curvature on plate penetration hole size caused by high-speed impact. Our intention is to quantify the effect of curvature on penetration hole diameter due to high-speed/hypervelocity impact of spherical projectiles into thin plates. It is important to be able to explain why body curvature has a minimal effect, and determine under what circumstances body curvature may become important. Use of a closed form analytical model is useful in determining trends and sensitivities of a particular effect, since one can directly observe the effect of a variable or parameter on the solution.

Following De Chant (2004a,b) and Appendix A the late time momentum conservation equation is modified to include external pressure effects caused by the shape of the curved body, e.g. a curved plate.

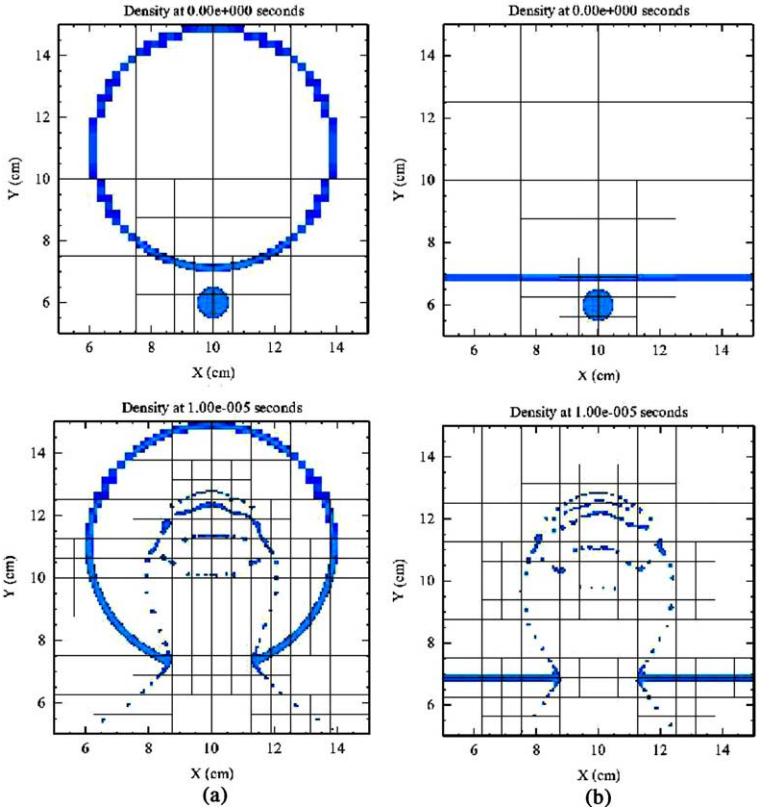

Fig. 1. Symmetric (about $x = 0$) impact of (a) a 1 cm diameter 6061-T6 aluminum sphere impacting a 8 cm diameter, 0.23 cm thick hollow 6061-T6 aluminum sphere and (b) a 1 cm diameter aluminum sphere impacting a 0.23 cm thick plate computed using the adaptive grid refinement AMR version of CTH. Impact velocity is 7 km/s.

Self-similarity of the momentum equation is admitted as before, however, the relationship is no longer homogeneous. The cross-stream flow equation is approximately solved to yield the late time penetration flow velocity field. Numerical inversion of a transcendental equation derived from the cross-steam flow solution gives a unique solution for the size of the curved plate penetration impact hole. The effect of the body curvature is reflected by the dimensionless plate thickness to radius of curvature of the parameter, h/R, which is naturally present in the transcendental equation. Several useful approximations to the transcendental equation solution are provided which explicitly show the effect of the h/R parameter and shows that curvature effects upon penetration hole diameter linearly scale with h/R. Thus we confirm that for most problems where a single layer shell (plate) can be meaningfully defined, the effect of curvature upon hole diameter is small, e.g. on the order of other modeling uncertainties, and is, therefore, negligible.

2. Analysis

Development of plate penetration hole diameter model begins by considering the following 2-d governing differential equations (White, 1991):

$$\begin{aligned}
&\rho_t + (\rho u)_x + (\rho v)_y = 0 \\
&u_t + uu_x + vu_y + \frac{1}{\rho}p_x = \nu_{\text{eff}}(u_{xx} + u_{yy}) \\
&v_t + uv_x + vv_y + \frac{1}{\rho}p_y = \nu_{\text{eff}}(v_{xx} + v_{yy})
\end{aligned} \tag{1}$$

where the effective viscosity relationship is a generalized function of velocity and length scales which is determined subsequently. A state relationship, e.g. $p = p(\rho, u)$ completes the system. The geometry associated with Eq. (1) is presented schematically in Fig. 2.

Unfortunately the system given in Eq. (1) is unsteady, non-linear and multidimensional and, as such, is not easily accessible using analytical methods. Further, we are interested in the late time, e.g. time independent behavior of the impact problem; solving the time dependent problem (except to obtain late time data) is not necessary nor desirable. Previously, De Chant (2004a,b) introduced a solution methodology that effectively overcomes these problems. The method involves (1) solving a reduced (1-d) unsteady equation for $u(x,t)$, (2) using the reduced to model the unsteady terms, e.g. u_t in the more complex, original equation and (3) solving the modified, now time independent, equation. Details of this analysis for a flat plat (that corresponds to an infinite radius of curvature which is equivalent to a finite radius problem for locations close to the stagnation point, i.e. $x \ll 1$ (see Fig. 2.)) are provided in Appendix A. In this paper, we apply a method related to that described in Appendix A, but extend the analysis to be valid for larger values of x.

Applying this methodology, see De Chant (2004a,b) and Appendix A for details, the modified system describing the impact problem is written:

$$\begin{aligned}
&u_x + v_y = 0 \\
&-\alpha u^2 + uu_x + vu_y = u\frac{\mathrm{d}U_{\mathrm{b}}}{\mathrm{d}x} + \frac{u}{\alpha}u_{yy}
\end{aligned} \tag{2}$$

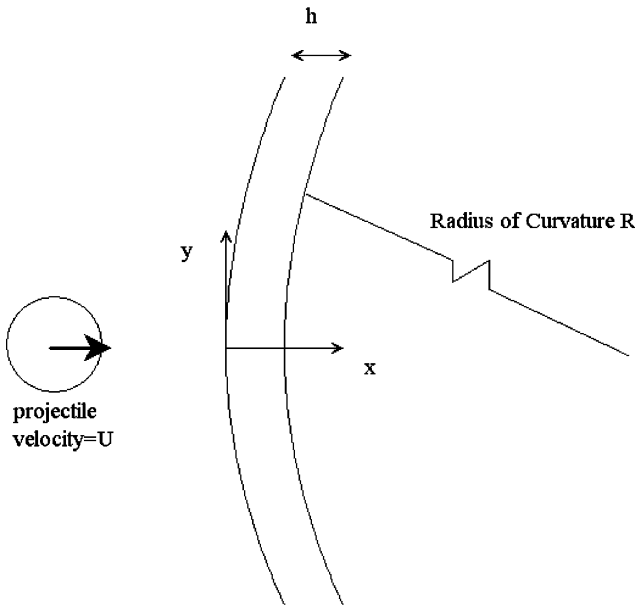

Fig. 2. Schematic of plate penetration impact problem.

Notice that unlike the flat plate model presented in Appendix A, a geometry/curvature dependent, pressure gradient term, e.g. $u\mathrm{d}U_\mathrm{b}/\mathrm{d}x$ is included in the formulation. This term follows by analogy with classical boundary layer methods where the pressure gradient is related to the flow via an inviscid Bernoulli's equation. Since the pressure gradient term, $u\mathrm{d}U_\mathrm{b}/\mathrm{d}x$ will introduce a new length scale associated with the geometry, i.e. the radius of curvature, a self-similar solution method as described in Appendix A will not be possible. However, as before, a stream function variable, $\psi(x,y)$ where $u = \partial\psi/\partial y$, $v = -\partial\psi/\partial x$ is defined which satisfies continuity and gives the single differential equation:

$$-\alpha(\psi_y)^2 + \psi_y\psi_{xy} - \psi_x\psi_{yy} = \psi_y\frac{\mathrm{d}U}{\mathrm{d}x} + \frac{\psi_y}{\alpha}\psi_{yyy} \tag{3}$$

Further, we recognize that $v \ll U$ thus, $|\psi_x| \ll 1$ and the term $\frac{\psi_x\psi_{yy}}{\psi_y}$ can be neglected. A more formal statement of this relationship implies that $\psi = Uy + \varepsilon_h\tilde{\psi}(x,y) + \cdots O(\varepsilon_h^2)$, where ε_h is a small parameter corresponding to dimensionless plate thickness, e.g. h/d, see Van Dyke (1975). The approximate expansion is thus only valid for thin plates where $u \approx U \gg 1$ and $v \ll 1$ (for very thick plates the flow field would be characterized by $u \approx v \approx O(1)$, this condition corresponding to a true stagnation point flow, see White (1991)).

$$-\alpha^2\tilde{\psi}_y + \alpha\tilde{\psi}_{xy} = \alpha\frac{\mathrm{d}U_\mathrm{b}}{\mathrm{d}x} + \tilde{\psi}_{yyy} \tag{4}$$

Several comments concerning Eq. (4) and its derivation are appropriate. The development of Eq. (4) differs from that given in Appendix A in that the term $\frac{\psi_x\psi_{yy}}{\psi_y}$ is neglected rather than modeled. Thus the final solutions achieved by solving Eq. (4) will be analogous to those in Appendix A, but formally different. The formulation of Eq. (4) should also be considered more approximate than the derivation given in Appendix A, however, for the purposes of this development where the focus is on the effect of curvature, Eq. (4) may be considered completely adequate. Notice, that the tilde designation is subsequently suppressed for economy of notation.

Although Eq. (4) cannot be self-similar due the presence of the term $\frac{\mathrm{d}U_\mathrm{b}}{\mathrm{d}x}$ and, therefore the separable self-similar equation used in Appendix A cannot be achieved, we can derive a non-similar solution based upon a powers series in "x" where the coefficient associated with each power is self-similar. There is a direct analogy between this proposed methodology and with boundary layer flow in the presence of a pressure gradient, such as flow over a cylinder, Schlicthing (1979).

Using the functional form of the self-similar equation derived by De Chant, i.e. $\psi = U\mathrm{e}^{-\alpha x}f(y)$ we write the non-similar expression:

$$\psi = U(1 - \alpha x + \cdots)(f_0(y) + xf_1(y) + \cdots) + O(x^2) \tag{5}$$

which permits computation of the stream function terms in Eq. (4). However to solve Eq. (4), the non-homogeneous term, $\mathrm{d}U/\mathrm{d}x$ must be expressible in terms of a power series as well. Consider for example, impact into a cylindrical shell. Following Schlicthing (1979) one finds that the flow $U_\mathrm{b}(x)$ is given as

$$U_\mathrm{b} = 2U\sin\left(\frac{x}{R}\right) = 2U\frac{x}{R} + \cdots O(x^2) \tag{6}$$

Substitution of Eqs. (5) and (6) into the simplified "u" momentum equation, e.g. Eq. (4) (recall that the continuity equation is automatically satisfied by the stream function definition) and collecting terms in powers of "x" gives

$$\begin{aligned} &f_0''' + 2\alpha^2 f_0' + 2\frac{\alpha}{R} - \alpha^2 = 0 + O(x) + \cdots \\ &f_1''' + 2\alpha^2 f_1' = 0 + O(x^2) + \cdots \end{aligned} \tag{7}$$

Eq. (7) is the basic differential equation for the curved wall impact problem and presents $O(1)$ and $O(x)$ solutions. The lowest order relationship contains the most important information, the $O(x)$ relationship being trivial (a homogeneous differential equation with homogeneous boundary conditions). As was the case for the self-similar flat plate problem, boundary conditions are $f_0(0) = 0$, $f_0'(0) = 1$ and $f_0'(\infty) = 0$. Solution of $f_0''' + 2\alpha^2 f_0' + 2\frac{z}{R} = 0$ yields

$$\begin{aligned} f_0' &= c_1 \cos\sqrt{2}\alpha y + c_2 \sin\sqrt{2}\alpha y - \frac{1}{\alpha R} \\ f_0 &= \frac{c_1}{\sqrt{2}\alpha} \sin\sqrt{2}\alpha y - \frac{c_2}{\sqrt{2}\alpha} \cos\sqrt{2}\alpha y - \frac{y}{\alpha R} + c_3 \end{aligned} \tag{8}$$

where c_1, c_2 and c_3 are integration constants to be defined via application of the boundary conditions. Applying boundary condition we write the relationship

$$f_0 = \frac{\left(1 + \frac{1}{\alpha R}\right)}{\sqrt{2}\alpha} \sin\sqrt{2}\alpha y - \frac{y}{\alpha R} \tag{9}$$

From Eq. (9) and stream function/velocity relationships we write

$$\begin{aligned} \psi &= \frac{U(\alpha R + 1)}{\sqrt{2}\alpha(\alpha R)} \sin\sqrt{2}\alpha y - \frac{y}{\alpha R} \\ u &= \psi_y = \frac{U(\alpha R + 1)}{(\alpha R)} \cos\sqrt{2}\alpha y - \frac{U}{\alpha R} \\ v &= -\psi_x = 0 + O(x^2) \end{aligned} \tag{10}$$

Eq. (10) is the late time (time independent) solution for the velocity field associated with the penetration of the thin plate with curvature as shown in Fig. 2. Notice, that Eq. (10) is analogous in form to the relationships in Appendix A but differs in detail, as previously indicated, a consequence of the approximations used to achieve Eq. (4).

As in De Chant (2004a) the major goal, however, is not to describe the velocity field associated with the plate hole penetration problem, but is to determine the size of the plate penetration hole. An estimate of this value can be obtained from the late time "v" velocity field. Indeed, the definition of $1/2$ the hole diameter is the "y" location at which the late time velocity, $v = 0$. Therefore, the roots associated with $\psi = 0$, define the critical y location (this follows from $\psi = U\mathrm{e}^{-\alpha x} f(y)$ rather than simply Eq. (4)):

$$\psi = \frac{U(\alpha R + 1)}{\sqrt{2}\alpha(\alpha R)} \sin\sqrt{2}\alpha y_{\text{crit}} - \frac{U y_{\text{crit}}}{\alpha R} \tag{11}$$

Alternatively we write the transcendental equation, $\sin\sqrt{2}\alpha y_{\text{crit}} - \frac{\sqrt{2}\alpha y_{\text{crit}}}{(\alpha R+1)} = 0$ which gives the critical location associated with maximum penetration hole size. For convenience we define, $\sqrt{2}\alpha y_{\text{crit}} \equiv \beta$. Recalling that from the flat plate problem that $\alpha = C_{\text{f}}/h$ we note that αR is proportional to the ratio of curvature to the plate thickness, i.e. $\alpha R \propto R/h$. Notice, that for $\alpha R \gg 1$, implying, the second term in the transcendental equation is small, that we recover $\sqrt{2}\alpha y_{\text{crit}} = \beta = \pi$ as computed for the flat plate case.

Following the previous model, the plate hole size is computed in a completely analogous manner, with the exception the eigenvalue π, is replaced by the result of the transcendental relationship, β. Thus we write

$$\frac{d_{\text{hole}}}{d} = 1 + \sqrt{2}\beta\left(\frac{h}{d}\right)\left(\frac{U}{c_{\text{wave}}}\right)^{1/2}\left(\frac{\rho_{\text{proj}}}{\rho_{\text{targ}}}\right)^{1/2} \tag{12}$$

where β is the zero of the equation.

$$\sin\beta - \frac{1}{\left(\frac{U}{c_{\text{wave}}}\right)^{-1/2}\frac{R}{h}+1}\beta = 0 \tag{13}$$

Eqs. (12) and (13) are the goal this paper. As expected from the form of Eq. (13), the effect of curvature is exhibited by the term $\frac{1}{\left(\frac{U}{c_{\text{wave}}}\right)^{-1/2}\frac{R}{h}+1}$ in Eq. (13). Defining $\frac{1}{\left(\frac{U}{c_{\text{wave}}}\right)^{-1/2}\frac{R}{h}+1} \equiv \varepsilon$, we can assess the effect of curvature on the root of Eq. (13), i.e. β and compare to the flat plate value, i.e. $\varepsilon = 0$ and $\beta = \pi$. The results of this comparison are presented in Fig. 3.

From Fig. 3 it is apparent that there is an approximately linear relationship between root β and the parameter ε in the solution of $\sin\beta - \varepsilon\beta = 0$. Though perhaps unexpected, that a linear relationship provides a reasonable approximation to the root, β, can be demonstrated by introducing the relationship $\beta = \pi + z(z \ll 1)$, expanding Eq. (13) in Taylor series and neglecting all but linear terms. This gives

$$\beta \approx \pi(1-\varepsilon) + O(\varepsilon^2, z^2) \tag{14}$$

Eq. (14) is plotted in Fig. 3. Note that although Eq. (14) demonstrates solution linearity, that it is only effective for $\varepsilon \lll 1$, a restriction consistent with the simple Taylor series expansion used here.

Notice that by utilizing the regression relationship presented in Fig. 3 that a completely explicit form for the penetration hole diameter in the presence of body curvature is obtained:

$$\frac{d_{\text{hole}}}{d} = 1 + \sqrt{2}(3.13 - 2.66\varepsilon)\left(\frac{h}{d}\right)\left(\frac{U}{c_{\text{wave}}}\right)^{1/2}\left(\frac{\rho_{\text{proj}}}{\rho_{\text{targ}}}\right)^{1/2} \tag{15}$$

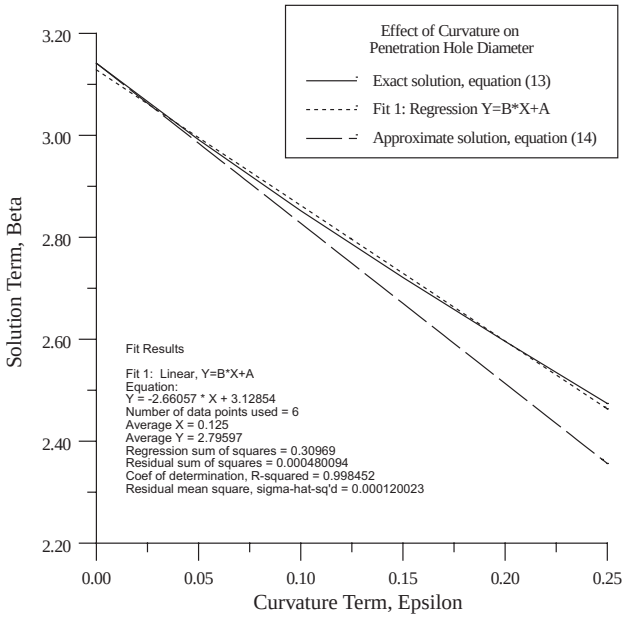

Fig. 3. Solution for β (also denoted as the dependent variable in the figure), see Eqs. (12) and (13), in terms of ε (defined in the text), a curvature dependent function. Notice the accuracy of the simple linear regression over the data range. The Taylor series approximation, i.e. Eq. (14), shows good accuracy for ε (also denoted as the independent variable in the figure) small.

where, ε is defined as before. Further by making the reasonable approximation that

$$\varepsilon = \frac{1}{\left(\frac{U}{c_{\text{wave}}}\right)^{-1/2}\frac{R}{h}+1} \approx \left(\frac{h}{R}\right)\left(\frac{U}{c_{\text{wave}}}\right)^{1/2} \tag{16}$$

and using Eq. (14), one can split the penetration hole diameter relationship into (I) and flat plate term and (II) a small (since we expect $h/R \ll 1$, while $U/c_{\text{wave}} = O(1)$) curvature correction, i.e.

$$\begin{aligned}\frac{d_{\text{hole}}}{d} &= 1+\sqrt{2}\pi\left(\frac{h}{d}\right)\left(\frac{U}{c_{\text{wave}}}\right)^{1/2}\left(\frac{\rho_{\text{proj}}}{\rho_{\text{targ}}}\right)^{1/2}\left[1-\left(\frac{h}{R}\right)\left(\frac{U}{c_{\text{wave}}}\right)^{1/2}\right] \\ &\approx 1+\sqrt{2}\pi\left(\frac{h}{d}\right)\left(\frac{U}{c_{\text{wave}}}\right)^{1/2}\left(\frac{\rho_{\text{proj}}}{\rho_{\text{targ}}}\right)^{1/2}+O\left[\left(\frac{h}{R}\right)\left(\frac{U}{c_{\text{wave}}}\right)^{1/2}\right]\end{aligned} \tag{17}$$

Thus, as one might expect the effect of curvature on penetration hole diameter is small and the experientially based statement, that "curvature has a minimal impact upon penetration hole diameter" is seen to be a quantitatively justified conclusion.

As a test of the conclusion that we have drawn from equation, namely that we consider several CTH based impact simulations. Similar to Fig. 1, we consider in Fig. 4 the impact of a solid, aluminum 6061-T6 sphere at 6.7 km/s striking a hollow, thickness 0.25 cm, aluminum 6061-T6 sphere. The CTH model for these problems utilizes a simple Mie-Gruneisen equation of state, EOS, and an elastic–plastic strength formulation (see Drumheller (1998) for discussion concerning EOS and strength formulations). The diameter of the target sphere is varied from 4–8 cm. For reference, an aluminum 6061-T6 plate (zero curvature) is also impacted. In complete accordance with Eq. (17), inspection of Fig. 4 indicates that the effect of target curvature on penetration hole diameter is minimal for the problems presented here, since even for impact, Fig. 4(a), the plate thickness to radius of curvature, h/R is small, i.e. 1/8. Further simulation results for increasing h/R indicate insensitivity to target curvature. Finally, by decreasing the radius of curvature further while keeping the thickness constant, one begins to approach the behavior a solid target and thus, it no longer makes sense to talk about plate penetration as presented here.

Numerical values for the impact problems presented in figure are summarized in Table 1. Notice that, as predicted by Eq. (17), that the penetration hole diameter is insensitive to the target's radius of curvature.

Fig. 4 and Table 1 combined with Eq. (17) provide a quantitative demonstration and explanation of the minimal effect that target curvature has on plate penetration hole diameter.

3. Conclusions

To develop a quantitative explanation for the minimal effect of curvature on penetration hole size we have developed an extension to a model developed by De Chant (2004a,b) to include the effects of body curvature on plate penetration hole size caused by hypervelocity impact for thin plates. The effect of curvature on penetration hole diameter is shown to scale linearly with h/R, the plate thickness to radius of curvature ratio. Thus we confirm that for most problems where a single layer shell can be meaningfully defined, the effect of curvature upon hole diameter is negligible.

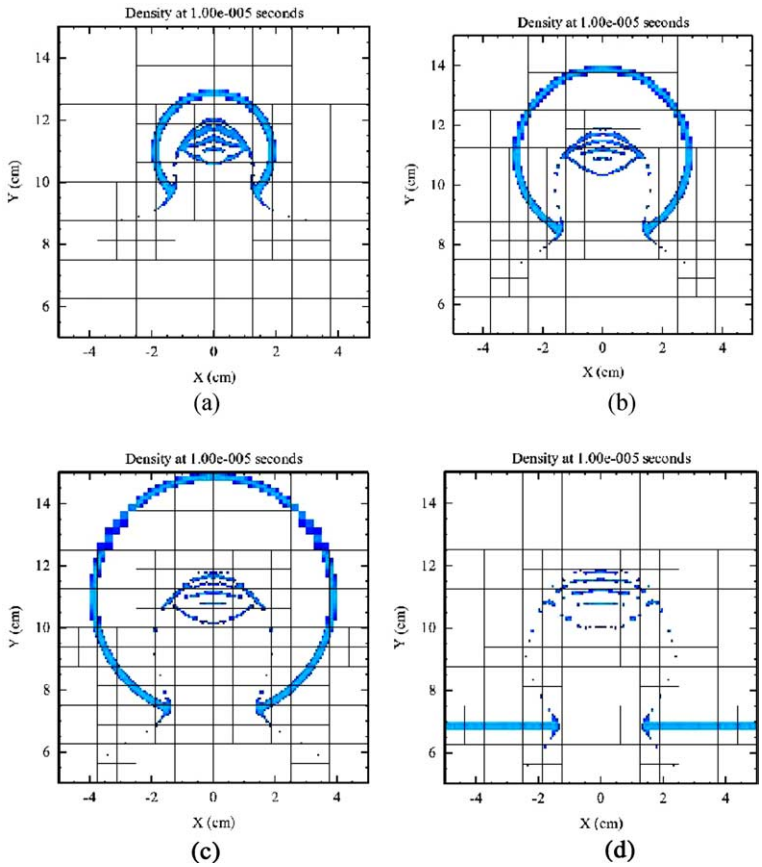

Fig. 4. Impact of a solid, 3 cm diameter aluminum 6061-T6 sphere at 6.7 km/s striking a hollow, thickness 0.25 cm, aluminum 6061-T6 sphere. The diameter of the target sphere is varied from 4, 6 and 8 cm, corresponding to (a)–(c), respectively. For reference, see (d), an aluminum 6061-T6 plate (zero curvature) is also impacted. Notice that the penetration hole diameter is approximately equal for all impacts.

Table 1
Comparison between penetration hole diameter as estimated by Eq. (17) and CTH simulation

Fig. 4 reference	Plate thickness/radius curvature; h/R	d_{hole}/d, Eq. (17)	d_{hole}/d; (CTH)	Percent relative error
(a)	0.125	1.32	1.20	10.0
(b)	0.0833	1.34	1.25	7.2
(c)	0.0625	1.35	1.28	5.5
(d)	0.0	1.37	1.32	3.8

Agreement ranges is good for all cases and supports the conclusion that curvature has a small influence on penetration hole diameter.

Acknowledgements

Encouragement from R. Schmitt, W. Erikson and E. Hertel Jr. of Sandia National Laboratory is appreciated. The insightful comments of an anonymous reviewer are appreciated. Sandia is a multi-program

Laboratory operated by Sandia Corporation, a Lockheed Martin Company for the United States Department of Energy under contract DE-AC04-94-AL85000.

Appendix A. Derivation of a hypervelocity plate penetration hole diameter relationship based on late time stagnation point flow concepts

In this appendix we derive a plate penetration hole diameter relationship using late time (steady) stagnation point flow concepts. This development closely parallels that provided in (De Chant, 2004a,b). The derivation provided will be a degenerate case of the curved plate relationship developed in the text. The flat plate penetration hole diameter solution shows good agreement with experimental data.

Starting with the system given in Eq. (1) and the nomenclature utilized in the text, we propose a solution strategy to simplify Eq. (1) and arrive at a valid, late-time approximate solution. This simplification process involves:

1. Solving a reduced (1-d) time dependent equation for $u(x,t)$.
2. Use the reduced solution to model the unsteady terms, e.g. u_t in the more complex, original equation.
3. Solve the modified, now time independent equation.

This strategy is implemented subsequently. The methodology described here is, of course, a particular case of a broad class of general iterative methods, Van Dyke (1975).

The appropriate, elementary model for the Eulerian treatment of high-speed flows, e.g. impact problems consists of the linear momentum conservation equation, De Chant, 2004c and Logan (1987):

$$u_t + uu_x + \frac{1}{\rho}p_x + \alpha u^2 = 0 \tag{A.1}$$

where α is a damping term with units $(1/L)$ and continuity. The damping length scale described here is related to the length scale mention previously associated with v_{eff} in Eq. (1). The 1-d unsteady continuity equation is written:

$$\rho_t + u\rho_x + \rho u_x = 0 \tag{A.2}$$

An additional relationship is designated to eliminate the pressure in terms of density and velocity by proposing a dynamic pressure closure of the form $p = k_0\rho u^2$. The term k_0 is considered constant. Using the form of a simple isentropic ideal gas (Whitham (1974)) one would write $k_0 = (\gamma M^2)^{-1}$ that for most high-speed impact problems implies that $k_0 = O(1)$. Note that many other materials, e.g. metals and solids exhibit similar behavior, Drumheller (1998). Eq. (1) is then written:

$$u_t + uu_x + k_0\left(\frac{u^2}{\rho}\rho_x + 2uu_x\right) + \alpha u^2 = 0 \tag{A.3}$$

As stated, our goal is to develop, an approximate kinematic wave, approximation for this system. We make the fundamental assumption that density rate of change with respect to time, ρ_t, may be modeled as $\rho_t \approx \rho u_x$, a quasi-steady approximation appropriate for convection dominated flows (De Chant, 2004d). Eq. (A.2) can now be re-written to yield:

$$\frac{u^2}{\rho}\rho_x = -2uu_x \tag{A.4}$$

and substituted into Eq. (A.3) gives:

$$u_t + uu_x + \alpha u^2 = 0 \tag{A.5}$$

Eq. (A.6) is the basic kinematic wave approximation considered in this development.

Given the initial condition, $u(x,0) = U = \text{constant}$ we can easily solve Eq. (A.5) using the method-of-characteristics, MOC, i.e. $\mathrm{d}u/\mathrm{d}t = -\alpha u^2$, along characteristics defined by $\mathrm{d}x/\mathrm{d}t = u$ to obtain, see Logan (1987), Whitham (1974) and Debnath (1997):

$$u(x,t) = \frac{U}{1+\alpha U t} \tag{A.6}$$

and the associated characteristic equation

$$\frac{\mathrm{d}x}{\mathrm{d}t} = u(x,t) \Rightarrow x = \frac{1}{\alpha}\ln(1+\alpha U t) \tag{A.7}$$

To this point it has been possible to use a set of exact (though 1-d) relationships to describe the kinematic wave propagation within a solid. To analyze the damping term, α, it becomes necessary to invoke a series of scaling arguments and analogies with classical viscous hydrodynamics, White (1991) and Schlicthing (1979). Though one might be tempted to criticize the use of this analogy as somewhat less rigorous than the preceding discussion, it is one of the goals of this discussion to show that basic fluid dynamics concepts are applicable to the penetration problem. Justification for the use of hydrodynamic concepts in hypervelocity impact problems is discussed in Walters and Zukas (1989) and Drumheller (1998) among others. As such, we will invoke a series of basic length and velocity scales appropriate to this problem, by drawing upon an analogy with classical fluid flow.

The fundamental length scale associated with the penetration problem is the plate thickness, h. If we postulate that $\alpha \approx C_\mathrm{f}/h$, we then have a dimensionally consistent definition for α, written in terms of the skin friction coefficient and plate thickness. Closure of the skin friction coefficient follows from classical boundary layer similarity analysis. Following White (1991), Schlicthing (1979) or Hughes and Brighton (1991) we assume that the skin friction coefficient can be written:

$$C_\mathrm{f} \propto \left(\frac{uh}{\nu}\right)^{-m} \tag{A.8}$$

Then by rearrangement and through the introduction of the friction velocity definition, we write:

$$\frac{u}{u_\tau} \propto \left(\frac{uh}{\nu}\right)^{\frac{m}{2-m}} \tag{A.9}$$

where u_τ is the friction velocity $(\tau/\rho)^{1/2}$ and ν is the kinematic viscosity. By assuming that the velocity field must be self-similar, e.g. $u/u_\tau \propto u/u_0$ we can write:

$$\frac{u}{u_0} = \left(\frac{y}{h}\right)^{\frac{m}{2-m}} \tag{A.10}$$

Classically, the exponent "m" ranges from 0.25 to 0.5 that denote turbulent pipe flow and laminar flow, respectively. For example, $m = 0.25$ denote the classical 1/7 power law profile, White (1991).

How can these relationships be adapted to the penetration flow of interest? First, we identify the appropriate velocity and length scales as being U and h. Also, we need an effective kinematic viscosity relationship. Here we consider the dimensions of the kinematic viscosity, i.e. (velocity)(length). Additionally, we expect that it is a material property. Two obvious material velocities are: a yield velocity $(Y_\mathrm{yield}/\rho)^{1/2}$ and the sound speed velocity c_wave. Though the yield velocity may be appropriate for lower velocity impacts, we expect that hypervelocity impacts are dominated by wave propagation speeds. As such, the effective dimensionless number for the penetration flow is simply $(u_0/c_\mathrm{wave}) = Re$. Especially near the head of the projectile, we expect that the flow is predominantly a laminar stagnation point system with a skin friction coefficient relationship of the form $C_\mathrm{f} = \text{const}/\sqrt{Re}$, White (1991) and Schlicthing (1979).

As such, within the laminar stagnation point boundary layer region, the appropriate similarity exponent is $m = 1/2$.

These arguments provide closure to the skin friction relationship. We can now write:

$$C_f \equiv 2\frac{\tau_{\text{penetration}}}{\rho u_0^2} \propto \left(\frac{u_0}{c_{\text{wave}}}\right)^{-m} \tag{A.11}$$

where m ranges from 1/2 to 1. To utilized Eq. (A.11) it is necessary to estimate a proportionality constant. Since we have no further information, we make the assumption that, as in Eq. (A.10), penetration stress $\tau_{\text{penetration}}$ is self-similar with respect to dynamic pressure, effectively setting the associated proportionality constant to unity.

Eq. (A.6) describe the 1-d, unsteady, $u = u(x,t)$, flowfield. It is not immediately apparent that the velocity field can be written as a function of "x" only, but by combining Eqs. (A.6) and (A.7) to eliminate the term $1 + \alpha U t$, we write:

$$u(x,t) = U\mathrm{e}^{-\alpha x} \tag{A.12}$$

Direct substitution of Eq. (A.12) into Eq. (A.1) indicates that the spatial varying relationship is truly a solution of the governing differential equation. Notice that Eq. (A.12) is completely time independent. The significance of Eq. (A.12) will be apparent subsequently.

We will now use the reduced solution to approximate unsteady behavior in system (1) and estimate an appropriate closure for the, as yet, unspecified effective viscosity. From the MOC solution, i.e. Eqs. (A.6) and (A.8) a model for $u_t = -\alpha u^2$ is immediately available. Finally the form of the damping term in Eq. (A.1) suggests that a suitable approximation for the effective viscosity in Eq. (1) is $\nu_{\text{eff}} = u/\alpha$. Notice that the velocity scale is the local velocity u rather than the initial impact velocity U and that the length scale is specified by the damping term α. As in Eq. (A.5), the streamwise pressure gradient, p_x, is assumed to be negligible. The processes of impact is dominated by flow coincident with the projectile path, as such, $u \gg v$, the hallmark of classical boundary/thin layer behavior. Following White (1991) and Schlicthing (1979) we neglect the plate coincident, "v" momentum equation and assume that $u_{xx} < u_{yy}$. These assumptions represent "standard" boundary layer approximations and are completely consistent with the fluid stagnation point problem. Finally the density behavior in the mass conservation relationship is ignored. The modified system describing the impact problem is then written:

$$\begin{aligned} &u_x + v_y = 0 \\ &-\alpha u^2 + u u_x + v u_y = \frac{u}{\alpha} u_{yy} \end{aligned} \tag{A.13}$$

To satisfy the continuity equation a stream function variable, $\psi(x,y)$ where $u = \partial\psi/\partial y$, $v = -\partial\psi/\partial x$ is defined. In a search for a self-similar solution for Eq. (A.13) we introduce the separation variable trial solution for $\psi(x,y) = a(x)f(y)$, in a manner completely analogous to the fluid flow stagnation problem, White (1991). Substitution of the trial solution into the "u" momentum equation (recall that the continuity equation is automatically satisfied by the stream function definition) gives:

$$-\alpha a^2 f'^2 + a a' f'^2 - a^2 f f'' = \frac{a^2}{\alpha} f' f''' \tag{A.14}$$

For a similarity solution to exist it is necessary for Eq. (A.14) to be independent of "x" or "y". Inspection of Eq. (A.14) will be independent of "x" if $aa' \propto a^2$. Notice though, that this proportionality is implied by Eq. (A.12) the lower order solution. Applying Eq. (A.12), e.g. $aa' = -\alpha a^2$ or $a(x) = U\mathrm{e}^{-\alpha x}$, Eq. (A.14) becomes (strictly dependent on "y" only):

$$f'f''' + 2\alpha^2 f'^2 + \alpha^2 ff'' = 0 \tag{A.15}$$

Eq. (A.15) is the self-similar equation governing impact/penetration flow velocities. This equation is reminiscent to the self-similar equation obtained for flow in a duct with porous walls, White (1991). Boundary conditions are $f(0) = 0$, $f'(0) = 1$ and $f'(\infty) = 0$. Again, we emphasize the consistency between the separation solution for $a(x)$ and Eq. (A.12).

Eq. (A.15) may be solved numerically or, by approximation, analytically. Since Eq. (A.15) is already approximate, it makes little sense to perform a precise numerical solution, especially since Dividing through by f' we see that the problem is linear except for the term $\frac{ff''}{f'}$. To simplify this equation we note that a particular solution (generally not of interest since it does not satisfy the boundary conditions) of Eq. (A.15) is $f = \text{const}$. Substitution of this particular solution into the non-linear term yields an indeterminate expression. If we postulate that this indeterminate expression is finite and is consistent in magnitude with the other terms in Eq. (16) we can write $\frac{ff''}{f'} \approx -1$. Note that one can also arrive at the closure $\frac{ff''}{f'} \approx -1$, by showing that a particular first order perturbation solution to $ff'' + f' = 0$, is given by $f = 1 - \varepsilon e^{-x} + \cdots$ Utilizing the relationship $\frac{ff''}{f'} \approx -1$, Eq. (A.15) becomes:

$$f''' + 2\alpha^2 f' = \alpha^2 \tag{A.16}$$

Solving Eq. (A.16) (which is non-homogeneous) gives the periodic solution $f' = c_1 \cos\sqrt{2}\alpha y + c_2 \sin\sqrt{2}\alpha y + \frac{1}{2}$ and $f = \frac{c_1}{\sqrt{2}\alpha} \sin\sqrt{2}\alpha y - \frac{c_2}{\sqrt{2}\alpha} \cos\sqrt{2}\alpha y + \frac{y}{2} + c_3$ where c_1, c_2 and c_3 are integration constants. Satisfaction of the boundary conditions gives:

$$\begin{aligned} f &= \frac{1}{2}\left(\frac{1}{\sqrt{2}\alpha}\sin\sqrt{2}\alpha y + y\right) \\ f' &= \frac{1}{2}(\cos\sqrt{2}\alpha y + 1) \end{aligned} \tag{A.17}$$

Applying the stream function/velocity relationships we write:

$$\begin{aligned} \psi &= \frac{U}{2\sqrt{2}\alpha} e^{-\alpha x}(\sin\sqrt{2}\alpha y + \sqrt{2}\alpha y) \\ u &= \psi_y = \frac{U}{2} e^{-\alpha x}(\cos\sqrt{2}\alpha y + 1) \end{aligned} \tag{A.18}$$

Eq. (A.18) is the late time (time independent) solution for the velocity field associated with the penetration of a thin flat plate. Eq. (A.18) contains the same information as the solution described in (De Chant, 2004a,b). For example, the radius of the penetration hole, defined as $y = y_{\text{crit}}$ is obtained by seeking the first root of the velocity, i.e. $u(y = y_{\text{crit}}) = \frac{U}{2} e^{-\alpha x}(\cos\sqrt{2}\alpha y_{\text{crit}} + 1) = 0 \Rightarrow \sqrt{2}\alpha y_{\text{crit}} = \pi$. This expression (and the closure expression for α) immediately leads to the penetration hole diameter relationship since:

$$\frac{d_{\text{hole}}}{d} = 1 + 2y_{\text{crit}} = 1 + \frac{\sqrt{2}\pi}{\alpha d} \tag{A.19}$$

giving

$$\frac{d_{\text{hole}}}{d} = 1 + \sqrt{2}\pi\left(\frac{h}{d}\right)\left(\frac{U}{c_{\text{wave}}}\right)^{1/2} \tag{A.20}$$

Extension to multiple density fields (different materials for penetrator and target plate) can be accommodated by introducing the density scaling relationship which comes directly from elementary boundary layer theory where density effects are included via a power-law relationship through the theoretically consistent the Illingsworth transformation or the Chapman–Rubesin parameter, White (1991), giving

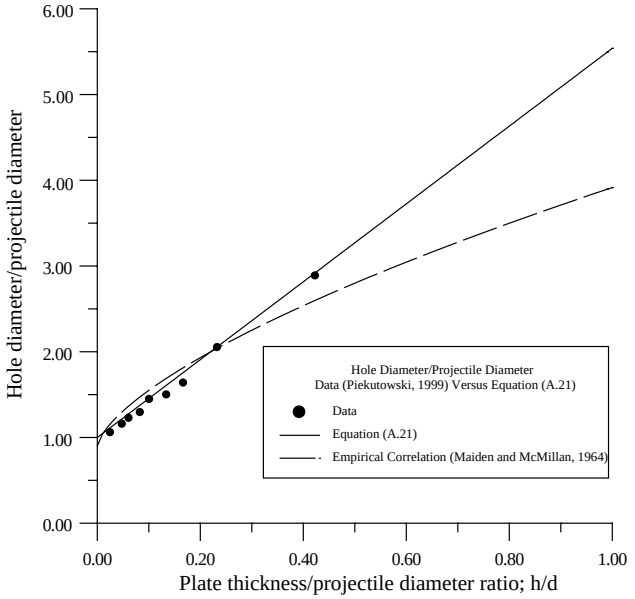

Fig. 5. Dimensionless penetration hole diameter as a function of plate thickness/projectile diameter, comparison with experiment, Piektukowski (1999) and correlation Maiden and McMillan (1964).

$$\frac{d_{\text{hole}}}{d} = 1 + \sqrt{2}\pi\left(\frac{h}{d}\right)\left(\frac{U}{c_{\text{wave}}}\right)^{1/2}\left(\frac{\rho_{\text{proj}}}{\rho_{\text{targ}}}\right)^{1/2} \tag{A.21}$$

Eq. (A.21) is the goal of the analysis presented in this appendix, a relationship describing the penetration hole diameter for a thin flat plate due to hypervelocity impact.

Comparison between the analytical result given by Eq. (A.21) and experimental measurements and numerical simulations are given in (De Chant, 2004a,b), while here we focus on the experimental results of Piektukowski (1999). Piektukowski (1999) provided a wealth of experimental data describing high Hypervelocity penetration hole problems. Data trends and comparison with empirical correlations, e.g. Maiden and McMillan (1964) are discussed in detail. Fig. 5 presents dimensionless penetration hole diameter as a function of plate thickness/projectile diameter ratio using experimentally measured values, the analytical model presented here, e.g. Eq. (A.21) and an empirical correlation, $d_{\text{hole}}/d = 0.45U(h/d)^{2/3} + 0.9$, U measured in Km/s (Maiden and McMillan (1964)). Examination of Fig. 5 indicates that Eq. (A.21) provides a good explanation for the data and provides the correct functional (linear) form. The correlation provides a less adequate model for $0 < h/d < 0.5$. The good agreement between experimental data and Eq. (A.21) provides confidence in the methodology developed here. The good agreement with experimental data, which is naturally 3-d, also confirms that the 2-d model developed here is completely adequate. (De Chant, 2004c) provides an additional mathematically-based explanation for this good agreement between 2-d modeling and 3-d experimental measurements.

References

Bell, R.L., Bauer, M.R., Brannon, R.M., Crawford, D.A., Elrick, M.G. Hertel Jr., E.S., Silling, S.A., Taylor, P.A., 2000. CTH Users Manual and Input Instructions, ver. 5.0, CTH Development Project, Sandia National Laboratories, November.

Corbett, G.C., Reid, S.R., Johnson, W., 1996. Impact loading of plates and shells by free-flying projectiles: a review. International Journal of Impact Engineering 18 (2), 141–230.

Debnath, L., 1997. Nonlinear Partial Differential Equations for Scientists and Engineers. Birkhauser, Boston.

De Chant, L.J., 2004a. A high velocity plate penetration hole diameter relationship based on late time stagnation point flow concepts, unpublished manuscript, Available from <ljdecha@sandia.gov>.

De Chant, L.J., 2004b. Validation of a computational implementation of the Grady–Kipp dynamic fragmentation theory for thin metal plate impacts using an analytical strain-rate model and hydrodynamic analogues. Mechanics of Materials, in press.

De Chant, L.J., 2004c. High velocity penetration depth relationships based on kinematic wave and elementary boundary layer concepts; support for empirical power law models. Advances in Space Research, submitted for publication.

De Chant, L.J., 2004d. A dynamic pressure/quasi-steady mass conservation approximation based kinematic wave model for high speed flows. International Journal of Nonlinear Mechanics, submitted for publication.

Drumheller, D.S., 1998. Introduction to Wave Propagation in Nonlinear Fluids and Solids. Cambridge University Press, NY.

Hughes, W.F., Brighton, J.A., 1991. Theory and Problems of Fluid Dynamics. McGraw-Hill, New York.

Logan, J.D., 1987. Applied Mathematics. New York, Wiley.

Maiden, C.J., McMillan, A.R., 1964. An investigation of the protection afforded a spacecraft by a thin shield. AIAA Journal 2 (11), 1992–1998.

McGlaun, J.M., Thompson, S.L., Elrick, M.G., 1990. CTH: A three-dimensional shock wave physics code. International Journal of Impact Engineering 10, 351–360.

Piektukowski, A.J., 1999. Holes produced in thin aluminum sheets by the hypervelocity impact of aluminum spheres. International Journal of Impact Engineering 23, 711–722.

Schlicthing, H., 1979. Boundary Layer Theory. New York, McGraw-Hill.

Van Dyke, M., 1975. Perturbation Methods in Fluid Mechanics. Parabolic Press, Stanford, CA, USA.

Walters, W.P., Zukas, J.A., 1989. Fundamentals of Shaped Charges. Wiley, New York.

White, F.M., 1991. Viscous Fluid Flow. McGraw-Hill, New York.

Whitham, G.B., 1974. Linear and Nonlinear Waves. Wiley, New York.